Appl. Phys. B 80, 857–860 (2005)
DOI: 10.1007/s00340-005-1805-6

Applied Physics B
Lasers and Optics

W. LIU[1,2,✉]
J.-F. GRAVEL[1]
F. THÉBERGE[1]
A. BECKER[2]
S.L. CHIN[1]

Background reservoir: its crucial role for long-distance propagation of femtosecond laser pulses in air

[1]Centre d'Optique, Photonique et Laser (COPL) and Département de Physique, de Génie Physique et d'Optique, Université Laval, Québec, Québec G1K 7P4, Canada
[2]Max-Planck-Institut für Physik komplexer Systeme, Nöthnitzer Strasse 38, 01187 Dresden, Germany

Received: 14 September 2004 /
Final version: 20 December 2004
Published online: 22 April 2005 •

ABSTRACT
We report an experiment to demonstrate the crucial effect of the so-called background reservoir during the propagation of femtosecond laser pulses in air. The background reservoir was blocked by allowing only the filament to pass through a pinhole generated by the filament itself in an aluminum foil. We observed that the filamentation process is terminated immediately after the pinhole. Consequently, to achieve long-range filamentation, it is necessary to maintain the dynamic energy exchange between the reservoir and the self-foci.

PACS 52.38.Hb; 42.65.Jx; 52.35.Mw

1 Introduction

Since its first observation in the 1990s [1–3], the phenomenon of laser pulse filamentation in air has been a hot topic because of its wide range of potential applications, such as pollutant detection [4] and lightning control [5–7]. The fundamental underlying mechanism of the filamentation process was concluded to be a dynamical balance between self-focusing induced by the optical Kerr effect and defocusing from the self-generated plasma in the self-focal region. On this basis, a self-waveguiding model was firstly proposed to explain the filamentation process [1, 2]. According to this model a waveguide is created due to the balance of self-focusing and defocusing, in which the laser beam propagates as a stable mode. Shortly after, an alternative scenario, namely the moving-focus model, was proposed by Brodeur et al. [3]. In this scenario each temporal slice of the laser pulse will self-focus at a different distance according to the power of the slice. As before, the radial collapse of the slice is arrested by the generation of plasma at high intensities. The succession of the self-foci creates a plasma channel, which is referred to as the 'filament'. The typical diameter of the self-foci is of the order of 100 μm in air [1–3] with a maximum clamped intensity around 5×10^{13} W/cm^2 [8–10].

The moving-focus model did not only account for the beginning of the filamentation process but also for the small ratio of the filament energy to the total energy observed in the experiments [3]. Indeed, it has been shown [3, 11] that the laser beam pattern recorded on a burn paper consists of a strong tiny spot, representing the self-focus, surrounded by a weaker background with a much larger diameter. The filament itself contains about 10% of the total energy only, while most of the energy is located in the background [3, 11]. This is consistent with the moving-focus model, in which the strong central spot arises from the slices that focus in the vicinity of this point, while the background arises from the majority of slices that focus at shorter or longer distances.

On the other hand, criticisms of the moving-focus model were brought forward by Lange et al. [12]. They showed that the filament in their experiment could persist beyond the linear focus in a focusing geometry. It seemed contrary to the moving-focus model, which implies that the filament should be terminated at the geometrical focus. However, Mlejnek et al. have advanced the preliminary moving-focus scenario to a dynamical spatial replenishment model [13, 14], in which they first presumed that the large-scale weak background is extending the filament through its re-focusing during the filamentation process. Several subsequent experiments provided further indications of the importance of the wide background for the formation of the ring structure [15, 16], during the transmission of the filament through clouds in the atmosphere [17] and for the re-focusing during pulse propagation [18, 19]. Recently, Kandidov et al. [20, 21] gave a detailed theoretical picture of the dynamic energy exchange process taking place between the tiny self-focus and the large background of the pulse, which influences the long-range filamentation of the femtosecond laser pulse. It gave rise to the concept of 'background reservoir' (also called 'energy reservoir').

In this paper, we report a simple experiment that confirms the crucial impact of the background reservoir on the filamentation process. To this end, we have blocked the wide background around the filament by a pinhole in an aluminum foil, created by the filament itself. The filamentation process is visualized by the observation of the fluorescence from excited

✉ Fax: +1-418-656-2623, E-mail: weliu@phy.ulaval.ca

nitrogen molecules generated in the plasma column. Our results show that without the reservoir the filament terminates immediately after the pinhole.

2 Experimental setup

In the experiments we used a commercial CPA (chirped pulse amplification) laser facility built by Spectra Physics. The system emits three simultaneous beams. It consists of an oscillator (Tsunami, 25 fs at 76 MHz), followed by a stretcher and a regenerative amplifier that works at 1-kHz repetition rate. A two-pass amplifier enhances the output from the regenerative amplifier. The amplified beam is compressed to 40 fs and gives a maximum energy of 2 mJ/pulse at 1 kHz. On the other hand, just after the regenerative amplifier, a pulse slicer is used to pick up one pulse every 100 ms. This 10-Hz seed beam is again split into two beams by a beam splitter. One part of the seed beam is sent to a two-pass amplifier and compressed by a portable compressor. After the portable compressor, 10-Hz laser pulses with an energy of 10 mJ/pulse and 42-fs duration are obtained. The second 10-Hz seed beam is sent to a four-pass amplifier, which is followed by a vacuum compressor. The output energy of this arm can be as high as 80 mJ/pulse having a duration of 45 fs. The three outputs are all centered at 800 nm and have a spectral bandwidth of 30 nm (FWHM). To perform the experiment reported here, we used the second output (i.e. 10 Hz, 10 mJ), which has a diameter of 6 mm at FWHM. The laser beam was focused by a 5-m focal length lens in air and a long filament was produced. In all the experiments, the laser pulse energy was set at 10 mJ, which corresponds to about 80 times the self-focusing critical power in air.

In the middle of the filament a piece of aluminum foil was inserted. First, the most intense part of the laser beam induced ablation of the aluminum foil and a hole was punched through the thin metal film. After the hole has been created and stabilized, it acts like a pinhole, which has a diameter determined by the transverse scale of the self-focus, for the following pulses. Thus, the weak background of the later pulses do not pass through the foil.

The detection system employed in this experiment is illustrated in Fig. 1a. An intensified CCD camera (ICCD, Princeton Instruments, PI-MAX 512) was applied to image the nitrogen molecule (N_2) and the nitrogen ion (N_2^+) fluorescence emitted from the filament. The nitrogen fluorescence has been proved to be generated in the plasma column [22] and is therefore a direct visualization of the filament [23]. A band-pass filter was placed in front of the camera (4-mm-thick UG11, Corion) to integrate the light emission over the strongest N_2/N_2^+ bands around 350 nm while rejecting the scattered light from the pump laser. There is a good overlap between the band-pass filter transmission curve and the strongest N_2/N_2^+ bands around 350 nm [23].

The fluorescence signal was collected and imaged onto the ICCD detector by using a single plano-convex lens made of fused silica with a focal length of 63 mm and a diameter of 38.1 mm. To allow the imaging of a long filament length, the ICCD system was installed in an off-axis configuration, at an angle of $\sim 45^\circ$ with respect to the laser propagation axis. With this configuration, about 2.5 m of the laser propagation axis

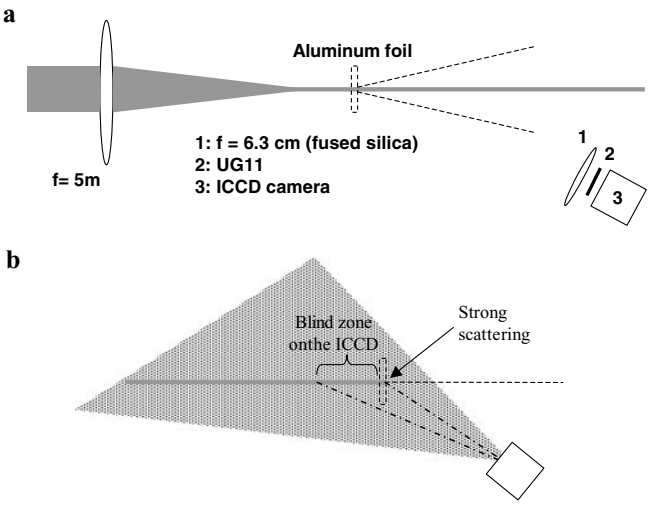

FIGURE 1 The experimental setup used to image the nitrogen fluorescence signal

was covered by the ICCD detection system. On the other hand, the geometry of the experimental setup shown in Fig. 1b elucidates that because of the off-axis configuration, the aluminum foil masks a small portion of the filament before the foil. The signal due to scattering from the pinhole is unavoidable.

The setup of the present experiment is similar to that of an earlier experiment [3], in which the moving-focus model was proved. But, the current setup differs from the previous one in two aspects, which are decisive for gaining a deeper understanding into the role of the wide background on the filamentation process. First, in the earlier experiment a prefabricated metal pinhole was used, which is replaced here by the laser self-created pinhole. Therefore, the new setup not only avoids the uncertainty of the pinhole alignment, but moreover the pinhole size is more precisely fitted to the rather sharp boundary between the intense spot of the filament and the much weaker pedestal of the background. Thus, the self-created pinhole blocks the wide background more efficiently. This certainly requires a high shot-to-shot stability of the laser system and of the filamentation process. We have therefore carefully observed that there was no significant change in the size of the ablated hole in the aluminium foil for interaction periods varying from 30 s up to 10 min. All our measurements are performed within that period. Second, instead of monitoring the filament energy passing through the pinhole [3], in the present experiment the filamentation process is visualized via the fluorescence measurement, which allows us to demonstrate visually and convincingly the effect of the background reservoir on the filamentation of the laser pulse along the propagation axis.

3 Results

In Fig. 2a we present the fluorescence picture taken by the ICCD camera for the filamentation process without the aluminum foil inserted into the beam. The picture is the result of a 1000-shot accumulation. The laser propagates from the left to the right of the picture. The scales are given in Fig. 2 and all distances are given with respect to the $f = 5$ m

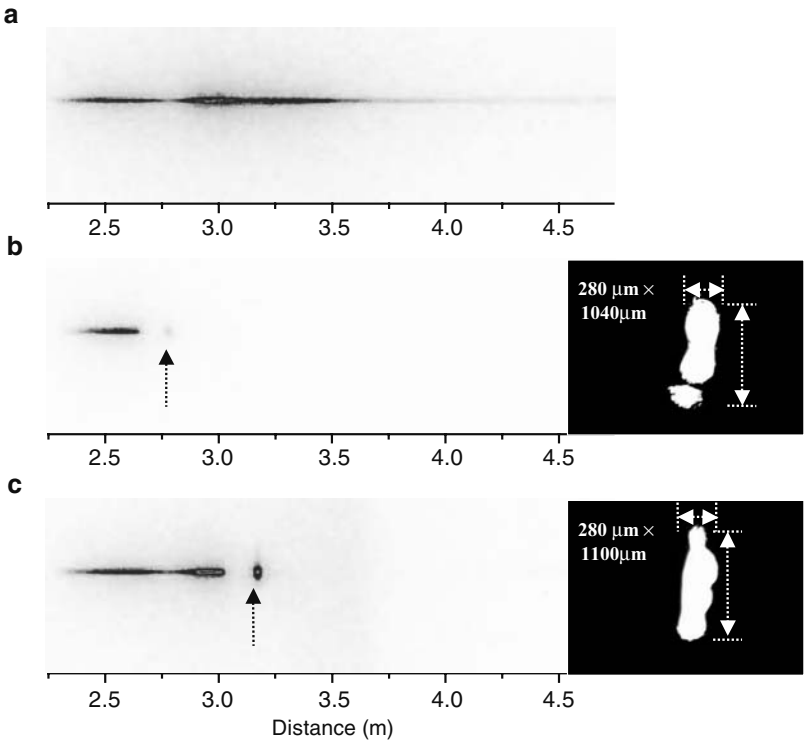

FIGURE 2 **a–c** Nitrogen fluorescence picture recorded by ICCD from the side of the propagation axis. **a** Without aluminum foil; **b** with aluminum foil at 2.75 m (*inset picture on right*: microscope image of the ablation pattern on the aluminum foil), the *arrow* indicates the position of the aluminum foil; **c** with aluminum foil at 3.15 m

focusing lens. It is seen from the figure that the onset of nitrogen fluorescence emission and, hence, the beginning of the filament occurs just after the laser pulse enters the field of view of the camera on the left-hand side. Along the propagation axis one can see two bright lines with a minimum in between, indicating re-focusing [9, 17], before the fluorescence signal slowly decreases towards the right-hand side of the picture, indicating the end of the filamentation process.

The fluorescence image shown in Fig. 2b was obtained with a piece of aluminum foil placed at 2.75 m behind the focusing lens; the position of the foil is indicated by the arrow. The inset on the right-hand side of the figure shows the image of the aluminum foil under the microscope (operated in the transmission mode) after being exposed to the laser beam. It shows three holes, two of them being connected. Each hole has a diameter of approximately 280 μm and the overall vertical dimension of the opening is slightly larger than 1 mm. The ablation pattern on the aluminum foil was similar to the single-shot beam pattern recorded by a burn paper. This shows that the multiple holes are not due to beam-pointing wandering but indicate the presence of multiple filaments. We should point out that the holes created through ablation have diameters larger than the reported filament size (i.e. the diameter of the plasma column). We relate it to the different nonlinear intensity dependences of the two processes. The ablation of the aluminum foil is a lower order intensity process compared to the multiphoton/tunnel ionization in air. It is reasonable that the ablation process will produce a larger-dimension hole than the filament itself. Thus, it is expected that a certain amount of energy of the background reservoir will leak through the larger hole. Even with that certain leakage of the background reservoir, the filamentation is stopped after the foil. It is in agreement with the results of one recent investigation, where it is shown that the self-focus, after being blocked, may regain energy from a background region exceeding 300 microns in diameter [24].

It should be noted parenthetically that a single filament could be achieved at lower laser energies in our experiment (a few times the self-focusing critical power). However, our laser beam mode is not good enough to maintain the single filament with increasing laser pulse energy. It will soon break up into multiple filaments. So far, we have not found a promising way to create a single filament at high energy. In the case of the single filament, the pulse is so weak that it is difficult to punch a hole in the aluminum foil. Therefore, we had to work with the multiple-filamentation case.

The fluorescence image in Fig. 2b visually agrees near the left-hand end with that obtained without insertion of the foil (panel a), but slightly before the position of the foil (at about 2.6 m) the signal is interrupted, followed by a single bright spot just behind the foil. Most interestingly, there is no fluorescence signal detected behind the foil (except for the bright spot); the second bright line, which is present in the case of the uninterrupted filamentation process, does not occur at all. Thus, there is no plasma generated behind the foil, suggesting that the filamentation process is obviously terminated by the foil. It should be noted that the decrease of the fluorescence intensity before the foil does not indicate a termination of the filament already, but it is just due to the experimental setup. As said before, the ICCD camera system is aligned at a certain angle with respect to the propagation axis. Part of the fluorescence emission (before the foil) will be masked by the foil, which was about 5 cm in width. It should be noticed that the bright spot near the location of the foil appears due to scattering generated from the pinhole ablated in the aluminum foil.

In order to show that this observation is not accidental, we have repeated the experiment with the aluminium foil placed at a different position, namely at 3.15 m. The corresponding

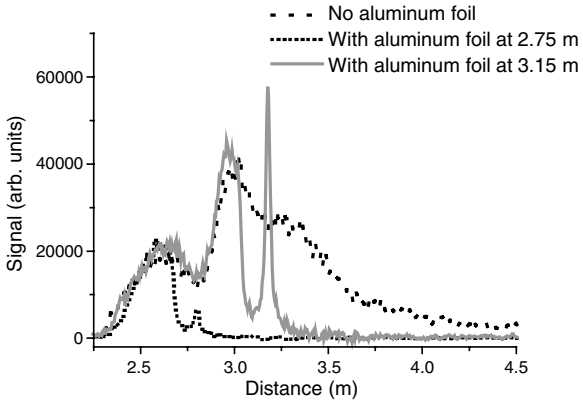

FIGURE 3 Plots of the nitrogen fluorescence signal distribution, integrated over the transverse direction, along the propagation distance. *Dotted line*: without aluminum foil, *short dotted line*: aluminum foil at 2.75 m, *solid line*: aluminum foil at 3.15 m

images of the florescence signal and of the aluminum foil after exposure to the beam are shown in Fig. 2c. We make the same observations as before; the fluorescence emission disappears behind the aluminum foil (its decrease before the foil followed by a single bright spot has the same reasons as above). The ablation pattern created at this position (right-hand inset) is similar to the one at the previous position. This time one can distinguish four holes indicating four filaments. The dimension of each hole is similar to those at the previous location, showing that each self-focus has a rather constant diameter during the propagation.

In Fig. 3 we present a quantitative comparison of the fluorescence signals integrated over the transverse direction, as a function of the propagation distance (after the focusing lens) for the three experiments shown in Fig. 2. One can first observe more clearly the modulation of the fluorescence intensity along the propagation axis for filamentation without the foil in the beam path (thick dotted line). By comparing the results obtained with and without the aluminum foil, it is seen that the integrated fluorescence intensity is essentially the same before the foil: up to the first maximum of the integrated fluorescence signal for the aluminum foil inserted at 2.75 m (thin dotted line) and up to the second maximum for the aluminum foil inserted at 3.15 m (solid line). Once the foil is inserted in the beam path and the pinhole is created, the integrated fluorescence signal quickly falls to the background level. This is an indication that the plasma density is decreased drastically to almost zero behind the aluminum foil, even though the most intense part of the pulse passed through the aluminum foil.

As mentioned before, the pinhole is self-created in the aluminum foil by the intense part of the beam. The pinhole dimension is determined by the intensity distribution across the self-focus at which the plasma is produced. Therefore, our experimental results clearly show that the filamentation process is terminated immediately when the weak background reservoir is blocked. This experimental observation leads to the conclusion that the filament formation over a long distance of propagation in air strongly depends on the field distribution localized in the background reservoir and its interaction with the field in the filament.

4 Conclusions

In summary, we have reported a simple experiment giving evidence of the crucial role of the reservoir of energy located in the wide background around the filament during femtosecond laser propagation. In the experiment, the background (energy) reservoir was blocked by an aluminum foil, while the self-focus passed through a self-generated pinhole in the foil. Under this condition the filamentation process, observed via fluorescence emission from the plasma column, was terminated immediately after the pinhole.

ACKNOWLEDGEMENTS This work was supported in part by NSERC, DRDC-Valcartier, Canada Research Chairs, CIPI, CFI and FQRNT. W. Liu is grateful for the hospitality he received at the Max-Planck-Institut für Physik komplexer Systeme.

REFERENCES

1 A. Braun, G. Korn, X. Liu, D. Du, J. Squier, G. Mourou, Opt. Lett. **20**, 71 (1995)
2 E.T.J. Nibbering, P.F. Curley, G. Grillon, B.S. Prade, M.A. Franco, F. Salin, A. Mysyrowicz, Opt. Lett. **21**, 62 (1996)
3 A. Brodeur, C.Y. Chien, F.A. Ilkov, S.L. Chin, O.G. Kosareva, V.P. Kandidov, Opt. Lett. **22**, 304 (1997)
4 J. Kasparian, M. Rodriguez, G. Mejean, J. Yu, E. Salmon, H. Wille, R. Bourayou, S. Frey, Y.-B. Andre, A. Mysyrowicz, R. Sauerbrey, J.-P. Wolf, L. Wöste, Science **301**, 61 (2003)
5 X.M. Zhao, J.-C. Diels, C.Y. Wang, J.M. Elizondo, IEEE J. Quantum Electron. **31**, 599 (1995)
6 H. Pépin, D. Comtois, F. Vidal, C.Y. Chien, A. Desparois, T.W. Johnston, J.C. Kieffer, B.L. Fontaine, F. Martin, F.A.M. Rizk, C. Potvin, P. Couture, H.P. Mercure, A. Bondiou-Clergerie, P. Lalande, I. Gallimberti, Phys. Plasmas **8**, 2532 (2001)
7 M. Rodriguez, R. Sauerbrey, H. Wille, L. Wöste, T. Fuji, Y.-B. André, A. Mysyrowicz, L. Klingbeil, K. Rethmeier, W. Kalkner, J. Kasparian, E. Salmon, J. Yu, J.-P. Wolf, Opt. Lett. **27**, 772 (2002)
8 J. Kasparian, R. Sauerbrey, S.L. Chin, Appl. Phys. B **71**, 877 (2000)
9 A. Becker, N. Aközbek, K. Vijayalakshmi, E. Oral, C.M. Bowden, S.L. Chin, Appl. Phys. B **73**, 287 (2001)
10 W. Liu, S. Petit, A. Becker, N. Aközbek, C.M. Bowden, S.L. Chin, Opt. Commun. **202**, 189 (2002)
11 S.L. Chin, A. Brodeur, S. Petit, O.G. Kosareva, V.P. Kandidov, J. Nonlinear Opt. Phys. Mater. **8**, 121 (1999)
12 H.R. Lange, G. Grillon, J.-F. Ripoche, M.A. Franco, B. Lamouroux, B.S. Sprade, A. Mysyrowicz, E.T.J. Nibbering, A. Chiron, Opt. Lett. **23**, 120 (1998)
13 M. Mlejnek, E.M. Wright, J.V. Moloney, Opt. Lett. **23**, 382 (1998)
14 M. Mlejnek, E.M. Wright, J.V. Moloney, IEEE J. Quantum Electron. **35**, 1771 (1999)
15 S.L. Chin, N. Aközbek, A. Proulx, S. Petit, C.M. Bowden, Opt. Commun. **188**, 181 (2001)
16 S.L. Chin, S. Petit, W. Liu, A. Iwasaki, M.-C. Nadeau, V.P. Kandidov, O.G. Kosareva, K.Yu. Andrianov, Opt. Commun. **210**, 329 (2002)
17 F. Courvoisier, V. Boutou, J. Kasparian, E. Salmon, G. Méjean, J. Yu, J.-P. Wolf, Appl. Phys. Lett. **83**, 213 (2003)
18 A. Talebpour, M. Abdel-Fattah, S.L. Chin, Opt. Commun. **183**, 479 (2000)
19 W. Liu, S.L. Chin, O. Kosareva, I.S. Golubtsov, V.P. Kandidov, Opt. Commun. **225**, 193 (2003)
20 V.P. Kandidov, O.G. Kosareva, A.A. Koltun, Quantum Electron. **33**, 69 (2003)
21 V.P. Kandidov, O.G. Kosareva, I.S. Golubtsov, W. Liu, A. Becker, N. Aközbek, C.M. Bowden, S.L. Chin, Appl. Phys. B **77**, 149 (2003)
22 A. Talebpour, S. Petit, S.L. Chin, Opt. Commun. **171**, 285 (1999)
23 S.A. Hosseini, Q. Luo, B. Ferland, W. Liu, N. Aközbek, G. Roy, S.L. Chin, Appl. Phys. B **77**, 697 (2003)
24 S. Skupin, L. Bergé, U. Peschel, F. Lederer, Phys. Rev. Lett. **93**, 023901 (2004)